Superconducting triangular islands as a platform for manipulating Majorana zero modes

Aidan Winblad[1] and Hua Chen[1,2]

[1] *Department of Physics, Colorado State University, Fort Collins, CO 80523, USA*

[2] *School of Advanced Materials Discovery, Colorado State University, Fort Collins, CO 80523, USA*

We study the possibility of obtaining robust Majorana zero modes (MZMs) at the corners of triangular superconducting islands, with the goal of finding alternative structures that can serve as building blocks for topological quantum computation. A spinless p-wave superconductor as a three point triangle, or triangular island, is consider in the presence of a vector potential field and we show it can be exactly solved to host MZMs on the corners. Additionally, for a hollow equilateral triangle subject to inhomogeneous supercurrents, from bulk-edge correspondence we find that MZMs can generally appear when two of the edges are of differing topological phase from the third edge. We also discuss the robustness of MZMs in possible experimental realizations of the triangular islands.

I. INTRODUCTION

For the past twenty years Majorana zero-modes (MZMs) in condensed matter systems have been highly sought after due to both its fault-tolerant topological protection and non-Abelian exchange statistics for quantum computating [1–5]. MZMs were originally proposed to be found in topological 2D p-wave superconducting vortices and at the ends of a topological 1D p-wave superconductor [6, 7]. A p-wave superconductor has yet to be discovered but innovative heterostructures have been proposed to make topological superconductors. Such systems make use of

s-wave superconductors in proximity to various heterostructures: topological insulator [8–11] or Josephson junction with in plane magnetic field [12–15], 2D electron gas (2DEG) with Rashba spin-orbit coupling (SOC) and ferromagnet [16–20], ferromagnetic atomic spin chains [21–23], and quantum anomalous Hall insulator (QAHI) [24–26]. There have been strides in potential measurements of MZMs, most of these focus on one end of the wire [27–38] looking at zero-bias conductance peak (ZBP) curves and more recently both ends of a wire [39]. A new potential measurement may soon help confirm the identity of MZMs using a quantum dot and crossed Andreev reflections (CAR) in a Josephson junction [40].

The main proposal to achieve braiding of MZMs uses 1D wires to create large networks of T-junctions to create tetrons and hexons. It is not a simple task to develop these networks [41] and proposed quasi-1D systems in thin films [42], a cross Josephson junction [43], or scissor cuts on a QAHI [26] to get around the difficult engineering of 1D wire networks. We propose an alternative structure by using triangular superconducting islands, which can be easily produced with epitaxial growth [44].

A common thread of the previous work has been to use a magnetic field or Zeeman effect to induce a topological phase transition. Takasan 2022 spends some time building up why one can use supercurrents, should we also talk about that or just reference their paper and the 2012 supercurrent paper and let that be good enough? Instead, it has been shown a supercurrent can induce a topological phase transtion in a given heterostructure [45, 46]. Adjusting the supercurrent can allow for manipulating the MZMs position along a wire. We show when using an inhomogeneous supercurrent on a minimal model MZMs can be exactly solved. Additionally, when using an inhomogeneous supercurrent on a quasi-1D or finite width hollow triangle island we can realize clean gap MZMs due to bulk-edge correspondence, calculating an approximate topological phase diagram with broad topological parameter regimes. Our platform allows for another

option to host and manipulate MZMs on triangular networks instead of 1D wire networks.

OUTLINE: (Sec I is . . . , Sec II is . . .)

II. MINIMAL TRIANGLE MODEL

We show exact MZMs are hosted in a minimal three site triangular lattice. Start with the Hamiltonian of a spinless or spin-polarized p-wave superconductor of a triangular lattice

$$\mathcal{H} = \sum_{\langle j,l \rangle} (-t c_l^\dagger c_j + \Delta e^{i\theta_{l,j}} c_l^\dagger c_j^\dagger + h.c.) - \sum_j \mu c_j^\dagger c_j, \tag{1}$$

where t is the hopping amplitude, Δ is the superconducting order parameter, μ is the chemical potential, $\theta_{l,j}$ is the angle between sites l and j. Next, a Peierls substitution is applied to the creation(annihilation) operators of the form

$$\begin{aligned} c_l^\dagger c_j &\to c_l^\dagger c_j \exp\left(-\frac{ie}{\hbar}\int_{r_j}^{r_l} \mathbf{A}\cdot d\mathbf{l}\right) \\ &\to c_l^\dagger c_j e^{i\phi_{l,j}}. \end{aligned} \tag{2}$$

Here the electron charge, e, and Planck's constant, $\hbar$, will be treated as natural numbers. One finds that t is the only term that picks up a phase, the modified Hamiltonian looks like

$$\mathcal{H} = \sum_{\langle j,l \rangle} (-t e^{i\phi_{l,j}} c_l^\dagger c_j + \Delta e^{i\theta_{l,j}} c_l^\dagger c_j^\dagger + h.c.) - \sum_j \mu c_j^\dagger c_j. \tag{3}$$

It is difficult to come to any conclusion while in the complex fermion basis, writing the Hamiltonian in a Majorana fermion basis shows a clearer picture. Maybe a see supplementary material XX for derivation here. The Hamiltonian now takes the form

$$\begin{aligned}\mathcal{H} = &-\frac{i\mu}{4}\sum_j (a_j b_j - b_j a_j) \\ &-\frac{i}{4}\sum_{\langle j,l\rangle}[(t\sin\phi_{l.j} - \Delta\sin\theta_{l,j})a_l a_j \\ &\quad +(t\sin\phi_{l,j} + \Delta\sin\theta_{l,j})b_l b_j \\ &\quad +(t\cos\phi_{l,j} + \Delta\cos\theta_{l,j})a_l b_j \\ &\quad -(t\cos\phi_{l,j} - \Delta\cos\theta_{l,j})b_l a_j]. \end{aligned} \tag{4}$$

The Hamiltonian is Hermitian if $\phi_{l,j} = -\phi_{j,l}$ and $\theta_{l,j} = \theta_{j,l} + \pi$.

We consider a three point triangular lattice, where each lattice point is a complex fermion housing two Majorana fermions. The bottom left point is a_1, b_1, bottom right is a_2, b_2, and the top point is a_3, b_3. Similar to Kitaev we will make the same assumptions $t = \Delta$ and $\mu = 0$. We are left with several combinations of trig terms, some of which are required to be zero. Notice the bottom row is a Kitaev chain, we need only to look at how the bottom row interacts with the top point. To achieve two MZMs at the bottom corners, let a_1 and b_2 be such modes. Anytime a_1 or b_2 appear in an equation its trig terms must cancel, eliminating these particles coupling from the rest of the system.

Looking at the coupling from site 1 to site 3, $\theta = \pi/3$, the first and last term are

$$(\sin\phi_{31} - \sin\pi/3)a_3a_1 = 0, \tag{5}$$

$$(\cos\phi_{31} - \cos\pi/3)b_3a_1 = 0. \tag{6}$$

This is true if $\phi_{31} = \pi/3$. Consider the coupling of site 3 to site 2, phase angle $\theta = -\pi/3$ and the two simplified equations involving b_2 are

$$(\sin\phi_{23} - \sin(\pi/3))b_2b_3 = 0,$$

$$(\cos\phi_{23} - \cos(\pi/3))b_2a_3 = 0,$$

thus $\phi_{23} = \pi/3$. A constant step-function vector potential can get the desired phase when

$$\mathbf{A} = \begin{cases} \dfrac{2\pi}{3\sqrt{3}a}\hat{\mathbf{y}} & x > 0 \\[2ex] \dfrac{-2\pi}{3\sqrt{3}a}\hat{\mathbf{y}} & x < 0. \end{cases} \tag{7}$$

We find this to be true when extrapulated from a three point triangle to a triangular island because we need only to consider how the the corner Majorana fermions couple with their neighboring sites. Calculating the energy spectrum for a full triangular island we found MZMs, however, they did not appear to live within a clean gap nor did they have a broad range of vector potential strengths hosting zero modes. Kitaev had noted one could still get a topological

phase for $-2t < \mu < 2t$ and MZMs hosting at the interface of differing topologies [7]. We would also like to find a range of chemical potentials and vector potential strengths that result in a topologically nontrivial phase. As a last note, any odd-function vector potential field can achieve exact MZMs on the bottom two vertices of a triangular island. We only consider constant vector potentials in the next section to allow for a fourier transform of the ribbons main axis.

III. TOPOLOGICAL PHASE DIAGRAM OF A FINITE WIDTH RIBBON

MZMs can be hosted at the end points of a chain with finite width as with a Josephson-junction or other thin films, provided the width is much smaller than the Majorana fermion decay length [12–15, 42]. Expanding on these ideas we would like to induce a topological phase transition for an infinite triangular lattice ribbon. This will help create an argument using bulk-edge correspondence to inform how MZMs will host at the interfaces of triangular island edges, i.e. their corners.

Starting from Eq. 3 and since we are interested how a finite width ribbon along the x-axis behaves in a constant vector field we will fourier transform along the x-axis only. Pick the following transform to be

$$c^{\dagger}_{m,n} = \frac{1}{\sqrt{N}} \sum_{k} c^{\dagger}_{k,n} e^{i\mathbf{k}\cdot\mathbf{r}_m} \tag{8}$$

where $\mathbf{k} = k\hat{\mathbf{x}}$ and $\mathbf{r}_m = ma\hat{\mathbf{x}}$, and for convenience a will be treated as a natural number. This leads to the following

block Hamiltonian

$$\mathcal{H}(k) = \frac{1}{2}\sum_k \Psi_k^\dagger \begin{pmatrix} \epsilon(k) & \delta(k) \\ \delta^\dagger(k) & -\epsilon(-k) \end{pmatrix} \Psi_k. \tag{9}$$

The $\epsilon(k)$ block is a tridiagonal with $\epsilon_0(k) = -2t\cos(k+\phi_1) - \mu$ along the diagonal, the upper diagonal is $\epsilon_1(k) = -t(e^{-i\phi_2} + e^{i(k-\phi_3)})$, and $\epsilon_1^*(k)$ along the lower diagonal. The $\delta(k)$ block is a tridiagonal with $\delta_0(k) = 2i\Delta\sin k$ along the diagonal, the upper diagonal is $\delta_1(k) = -\Delta(e^{i\theta_2} + e^{i(k+\theta_3)})$, and $-\delta_1(-k)$ along the lower diagonal. The size of each block is the number of rows along the y-axis in a ribbon.

To calculate the Majorana number (M) the Hamiltonian needs to be in skew-symmetric form. One such way is to write it in the Majorana fermion basis, the transformation matrix is of the form

$$u = \frac{1}{\sqrt{2}} \begin{pmatrix} 1 & 1 \\ -i & i \end{pmatrix} \tag{10}$$

To account for the finite number of rows in a ribbon include a tensor product with an identity matrix of the same size, $U = u \otimes I_n$. We arrive at the skew-symmetric matrix with the following equation

$$A_{ch} = -iU\mathcal{H}_{ch}U^\dagger. \tag{11}$$

The $\mathcal{M}$ of a 1D chain is defined as

$$\mathcal{M} = \text{sgn}[\text{Pf}(A_{ch})], \tag{12}$$

where Pf stands for the Pfaffian of a skew-symmetric matrix [7]. We make the claim this satisfies a finite width ribbon as well. When $\mathcal{M} = -1$, the ribbon is in a nontrivial topology and expect MZMs at its edges. Sweeping through a range of A for the vector potential we expect to see a gap closing, $\mathcal{M} = 1$, and the system take on a trivial topology, no Majorana zero modes would exist on the edge of a finite ribbon.

To illustrate the importance of bulk-edge correspondence in forming Majorana fermions we will now look at the edges of a hollow triangular island. We show the top edges can be in a trivial phase while the bottom remains in a nontrivial phase. In previous papers a constant vector potential was used along the chain's axis [45, 46]. We instead use a constant vector potential step function from the previous section centered on a chain with two 60 degree bends, equating it to a equilateral triangle. Taking a hollow triangular island centered about the y-axis with the following vector potential

$$\mathbf{A} = \begin{cases} A\hat{\mathbf{y}} & x > 0 \\ \\ -A\hat{\mathbf{y}} & x < 0 \end{cases} \tag{13}$$

we examine each edge individually. When calculating M the vector potential has symmetry about the ribbon's axis, i.e. $\mathbf{A}$ pointing in the positive or negative y-axis yields the same result. Looking at Fig. 1 we determine each edge's

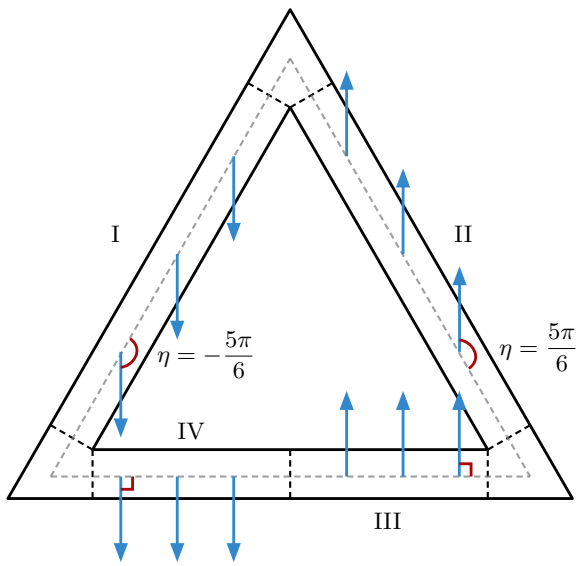

FIG. 1. Triangular island with constant step function vector potential. The edges are divided up into four regions with differing vector potentials. Each segment is treated like a finite width ribbon where we can test its topology as function of μ and $\mathbf{A}$. Vector potential $\mathbf{A}$ makes an angle $\eta = \mp\frac{5\pi}{6}, \pm\frac{\pi}{2}$, to each ribbon's main axis, respectively.

vector potential with respect to its main axis.

The topological phase diagram for ribbons III and IV, with three rows, can be seen in Fig. 2a, we can see for varying μ and A, with $\mathbf{A} = A\hat{\mathbf{y}}$, the system is topologically trivial (yellow) and nontrivial (blue). It appears when the vector potential is perpendicular to the ribbon it does not contribute to the topology of the system. Similarly, for ribbons I and II, with three rows, the topological phase diagram is seen in Fig. 2b. Here the vector potential plays a vital role in transitioning the topology.

We make use of bulk-edge correspondence to justify MZMs hosting at the interfaces of the triangular islands edges, i.e. corners. One simulataneously tunes regions I and II to be in a trivial(nontrivial) topological phase and regions III and IV to be nontrivial(trivial) topological phase, respectively. To check we look at an eigenenergy spectral flow and eigenstates of a triangular lattice with size $n = 100$, width $w = 3$, and $A = [0, 2\pi]$. Fig. 3 shows strong agreement

FIG. 2. Topological phase diagrams for a system with three rows (a) regions III and IV, and (b) regions I and II, from Fig. 1

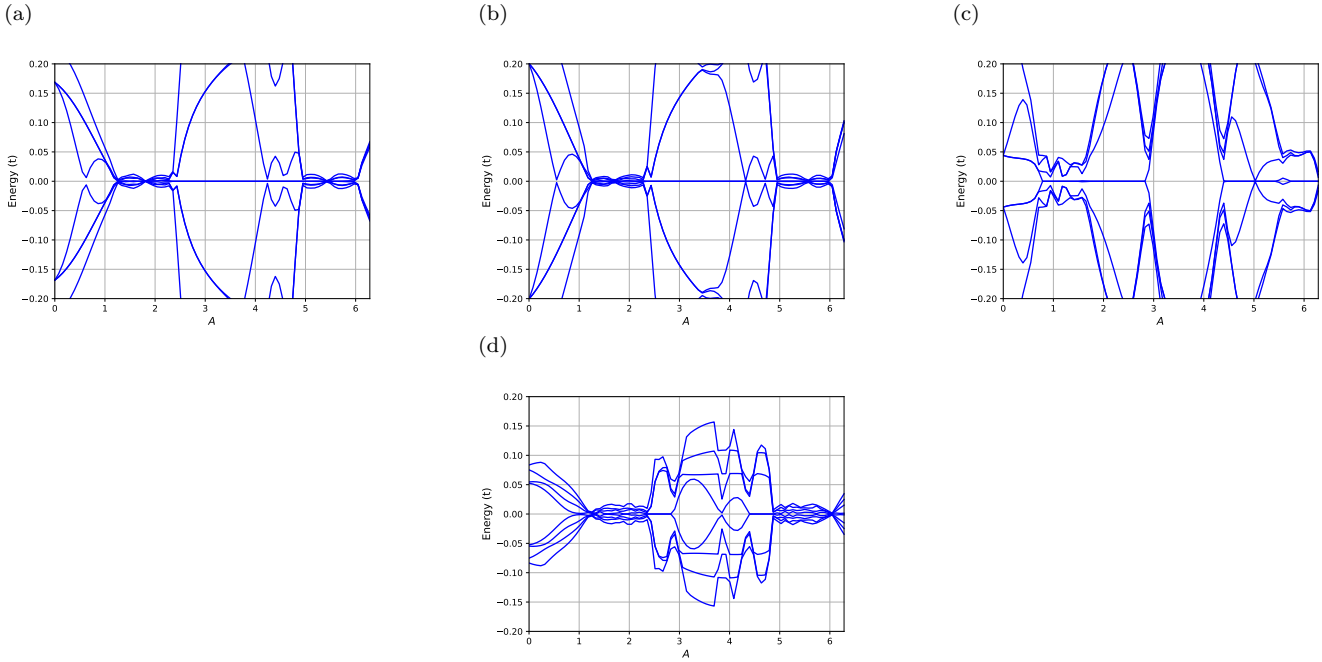

FIG. 3. Eigenenergy spectral flow for a system with $n_r = 100$ and $w_{edge} = 3$, with (a) $\mu = 0$, (b) $\mu = 0.2t$, (c) $\mu = 1.6t$, and (d) $\mu = -1.6t$.

of MZMs appearing in the same vector potential range as seen in Fig. 2b's topological phase diagram. As expected MZMs host at the bottom corners of the triangle where the differing topologies meet, as seen in Fig. 4. We see a broad parameter space, μ and A, for our system to host MZMs. Our calculations also show the MZMs live within a clean gap inside those parameter ranges.

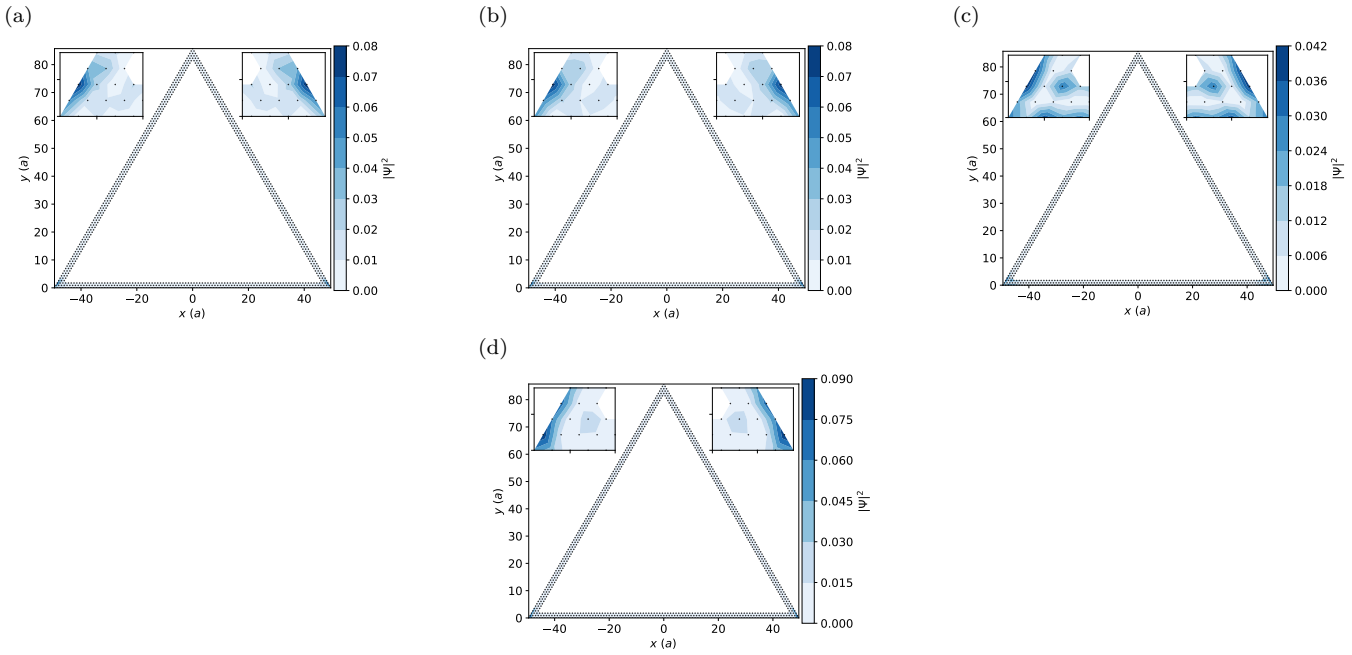

FIG. 4. MZMs for a system with $n_r = 100$ and $w_{edge} = 3$, with (a) $\mu = 0.2t$, $A = 2.8274$, (b) $\mu = 0.2t$, $A = 2.5918$, (c) $\mu = 1.6t$, $A = 2.6704$, and (d) $\mu = -1.6t$, $A = 2.4347$.

IV. DISCUSSION AND CONCLUSIONS

How one can build this system warrants some thought. A minimal model may be achieved by using a mesoscopic model involving quantum dots at the triangles vertices, to represent the minimal three point model [47]. If using epitaxial growth [44] one could make a network of vertex connected triangles, then either hollow the triangle out using ablation techniques or place a smaller inner voltage gates to tune the chemical potential to be a very strong trivial superconductor. One could place individual atoms using an STM tip [39]. Another option may be to use quasi-1D cuts on a QAHI with triangular lattice in proximity to an s-wave superconductor [26]. To implement the inhomogeneous supercurrent or vector potential one could use a magnetic field and a uniform supercurrent or two antiparallel supercurrents separated by a 1D or quasi-1D insulator strip. To braid MZMs in this system one only has to rotate and slowly turn on neighboring triangles inhomogeneous vector potentials to transition an edge to be of

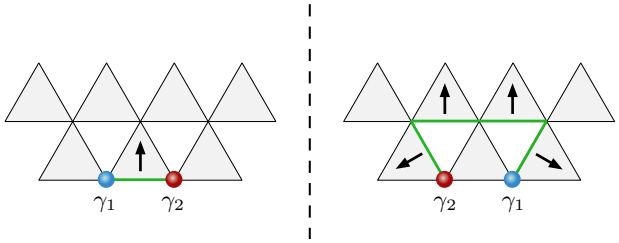

FIG. 5. Network of tunable topological superconducting hollow triangular islands. The left panel shows the initialization of two MZMs γ_1 and γ_2. The right panel depicts the MZMs after a braiding operation. The arrows depict which island has an inhomogeneous vector potential applied and in general direction for a step-function. Green lines shows which edges are topologically nontrivial.

nontrivial topology. The following schematic in Fig. 5 illustrates how such a manipulation of MZMs can occur.

With the base model for a new platform displayed further work is still required. A description of the Wannier states would be informative (Hua, I'm not well versed in this type of description, could use your expertise here in writing this sentence as it sounds important to include). Perfectly fabricated devices are not always realistic, a further study of the effects misshapen lattice edges would be important to further gauge how robust our platform is. Another calculation of how the MZMs evolve on a single triangle when the vector potential is rotated by 2π at its center would be informative if they survive such a process without mixing into higher order states and if they pick up a phase accumulation.

ACKNOWLEDGMENTS

Supported by XYZ Grant No. XXXXXX etc.

[1] D. A. Ivanov, Phys. Rev. Lett. **86**, 268 (2001).

[2] A. Yu. Kitaev, Annals of Physics **303**, 2 (2003).

[3] C. Nayak, S. H. Simon, A. Stern, M. Freedman, and S. Das Sarma, Rev. Mod. Phys. **80**, 1083 (2008).

[4] J. Alicea, Y. Oreg, G. Refael, F. von Oppen, and M. P. A. Fisher, Nature Phys **7**, 412 (2011).

[5] D. Aasen, M. Hell, R. V. Mishmash, A. Higginbotham, J. Danon, M. Leijnse, T. S. Jespersen, J. A. Folk, C. M. Marcus, K. Flensberg, and J. Alicea, Phys. Rev. X **6**, 031016 (2016).

[6] N. Read and D. Green, Phys. Rev. B **61**, 10267 (2000).

[7] A. Y. Kitaev, Phys.-Usp. **44**, 131 (2001).

[8] L. Fu and C. L. Kane, Phys. Rev. Lett. **100**, 096407 (2008).

[9] P. Hosur, P. Ghaemi, R. S. K. Mong, and A. Vishwanath, Phys. Rev. Lett. **107**, 097001 (2011).

[10] A. C. Potter and P. A. Lee, Phys. Rev. B **83**, 184520 (2011).

[11] M. Veldhorst, M. Snelder, M. Hoek, C. G. Molenaar, D. P. Leusink, A. A. Golubov, H. Hilgenkamp, and A. Brinkman, physica status solidi (RRL) – Rapid Research Letters **7**, 26 (2013).

[12] A. M. Black-Schaffer and J. Linder, Phys. Rev. B **84**, 180509 (2011).

[13] F. Pientka, A. Romito, M. Duckheim, Y. Oreg, and F. von Oppen, New J. Phys. **15**, 025001 (2013).

[14] M. Hell, M. Leijnse, and K. Flensberg, Phys. Rev. Lett. **118**, 107701 (2017).

[15] B. Scharf, F. Pientka, H. Ren, A. Yacoby, and E. M. Hankiewicz, Phys. Rev. B **99**, 214503 (2019).

[16] Y. Oreg, G. Refael, and F. von Oppen, Phys. Rev. Lett. **105**, 177002 (2010).

[17] J. D. Sau, R. M. Lutchyn, S. Tewari, and S. Das Sarma, Phys. Rev. Lett. **104**, 040502 (2010).

[18] R. M. Lutchyn, T. D. Stanescu, and S. Das Sarma, Phys. Rev. Lett. **106**, 127001 (2011).

[19] A. C. Potter and P. A. Lee, Phys. Rev. B **85**, 094516 (2012).

[20] S. Nadj-Perge, I. K. Drozdov, B. A. Bernevig, and A. Yazdani, Phys. Rev. B **88**, 020407 (2013).

[21] T.-P. Choy, J. M. Edge, A. R. Akhmerov, and C. W. J. Beenakker, Phys. Rev. B **84**, 195442 (2011).

[22] B. Braunecker and P. Simon, Phys. Rev. Lett. **111**, 147202 (2013).

[23] J. Klinovaja, P. Stano, A. Yazdani, and D. Loss, Phys. Rev. Lett. **111**, 186805 (2013).

[24] C.-Z. Chen, Y.-M. Xie, J. Liu, P. A. Lee, and K. T. Law, Phys. Rev. B **97**, 104504 (2018).

[25] Y. Zeng, C. Lei, G. Chaudhary, and A. H. MacDonald, Phys. Rev. B **97**, 081102 (2018).

[26] Y.-M. Xie, X.-J. Gao, T.-K. Ng, and K. T. Law, Creating Localized Majorana Zero Modes in Quantum Anomalous Hall Insulator/Superconductor Heterostructures with a Scissor (2021), arxiv:arXiv:2012.15523.

[27] V. Mourik, K. Zuo, S. M. Frolov, S. R. Plissard, E. P. A. M. Bakkers, and L. P. Kouwenhoven, Science **336**, 1003 (2012).

[28] L. P. Rokhinson, X. Liu, and J. K. Furdyna, Nature Phys **8**, 795 (2012).

[29] M. T. Deng, C. L. Yu, G. Y. Huang, M. Larsson, P. Caroff, and H. Q. Xu, Nano Lett. **12**, 6414 (2012).

[30] S. Nadj-Perge, I. K. Drozdov, J. Li, H. Chen, S. Jeon, J. Seo, A. H. MacDonald, B. A. Bernevig, and A. Yazdani, Science **346**, 602 (2014).

[31] J.-P. Xu, M.-X. Wang, Z. L. Liu, J.-F. Ge, X. Yang, C. Liu, Z. A. Xu, D. Guan, C. L. Gao, D. Qian, Y. Liu, Q.-H. Wang, F.-C. Zhang, Q.-K. Xue, and J.-F. Jia, Phys. Rev. Lett. **114**, 017001 (2015).

[32] S. M. Albrecht, A. P. Higginbotham, M. Madsen, F. Kuemmeth, T. S. Jespersen, J. Nygård, P. Krogstrup, and C. M. Marcus, Nature **531**, 206 (2016).

[33] H.-H. Sun, K.-W. Zhang, L.-H. Hu, C. Li, G.-Y. Wang, H.-Y. Ma, Z.-A. Xu, C.-L. Gao, D.-D. Guan, Y.-Y. Li, C. Liu, D. Qian, Y. Zhou, L. Fu, S.-C. Li, F.-C. Zhang, and J.-F. Jia, Phys. Rev. Lett. **116**, 257003 (2016).

[34] D. Wang, L. Kong, P. Fan, H. Chen, S. Zhu, W. Liu, L. Cao, Y. Sun, S. Du, J. Schneeloch, R. Zhong, G. Gu, L. Fu, H. Ding, and H.-J. Gao, Science **362**, 333 (2018).

[35] B. Jäck, Y. Xie, J. Li, S. Jeon, B. A. Bernevig, and A. Yazdani, Science **364**, 1255 (2019).

[36] A. Fornieri, A. M. Whiticar, F. Setiawan, E. Portolés, A. C. C. Drachmann, A. Keselman, S. Gronin, C. Thomas, T. Wang, R. Kallaher, G. C. Gardner, E. Berg, M. J. Manfra, A. Stern, C. M. Marcus, and F. Nichele, Nature **569**, 89 (2019).

[37] H. Ren, F. Pientka, S. Hart, A. T. Pierce, M. Kosowsky, L. Lunczer, R. Schlereth, B. Scharf, E. M. Hankiewicz, L. W. Molenkamp, B. I. Halperin, and A. Yacoby, Nature **569**, 93 (2019).

[38] S. Manna, P. Wei, Y. Xie, K. T. Law, P. A. Lee, and J. S. Moodera, Proceedings of the National Academy of Sciences **117**, 8775 (2020).

[39] L. Schneider, P. Beck, J. Neuhaus-Steinmetz, L. Rózsa, T. Posske, J. Wiebe, and R. Wiesendanger, Nat. Nanotechnol. **17**, 384 (2022).

[40] G.-H. Feng and H.-H. Zhang, Phys. Rev. B **105**, 035148 (2022).

[41] T. Karzig, C. Knapp, R. M. Lutchyn, P. Bonderson, M. B. Hastings, C. Nayak, J. Alicea, K. Flensberg, S. Plugge, Y. Oreg, C. M. Marcus, and M. H. Freedman, Phys. Rev. B **95**, 235305 (2017).

[42] A. C. Potter and P. A. Lee, Phys. Rev. Lett. **105**, 227003 (2010).

[43] T. Zhou, M. C. Dartiailh, W. Mayer, J. E. Han, A. Matos-Abiague, J. Shabani, and I. Žutić, Phys. Rev. Lett. **124**, 137001 (2020).

[44] O. Pietzsch, S. Okatov, A. Kubetzka, M. Bode, S. Heinze, A. Lichtenstein, and R. Wiesendanger, Phys. Rev. Lett. **96**, 237203 (2006).

[45] A. Romito, J. Alicea, G. Refael, and F. von Oppen, Phys. Rev. B **85**, 020502 (2012).

[46] K. Takasan, S. Sumita, and Y. Yanase, Phys. Rev. B **106**, 014508 (2022).

[47] T. Dvir, G. Wang, N. van Loo, C.-X. Liu, G. P. Mazur, A. Bordin, S. L. D. ten Haaf, J.-Y. Wang, D. van Driel, F. Zatelli, X. Li, F. K. Malinowski, S. Gazibegovic, G. Badawy, E. P. A. M. Bakkers, M. Wimmer, and L. P. Kouwenhoven, Nature **614**, 445 (2023).